

## Finite-size and dynamical effects in pair production by an external field

Cécile Martin and D. Vautherin

*Division de Physique Théorique, Institut de Physique Nucléaire, F-91406 Orsay, CEDEX, France*

(Received 3 January 1989)

We evaluate the rate of pair production in a uniform electric field confined to a bounded region in space. Using the Balian-Bloch expansion of Green's functions we obtain explicit expressions for finite-size corrections to Schwinger's formula. The case of a time-dependent boundary, relevant to describe energy deposition by quark-antiquark pair production in ultrarelativistic collisions, is also investigated. We find that finite-size effects are important in nuclear collisions. They decrease when the strength of the chromoelectric field between the nuclei is large. As a result, the rate of energy deposition increases sharply with the mass number  $A$  of the colliding nuclei.

### I. INTRODUCTION

The production of fermion-antifermion pairs by a classical external field via the so-called Schwinger mechanism<sup>1</sup> is a very general phenomenon. It occurs in a rather wide variety of problems and has been the subject of a large number of studies (cf. the comprehensive review paper by Soffel, Müller, and Greiner<sup>2</sup>).

One example, originally discussed by Schwinger, is the problem of electron-positron pair creation out of the Dirac vacuum due to a strong electric field. In this case the pair-production rate is expected to be significant whenever the strength  $eE$  of the electric field becomes comparable to the square of the electron mass. This condition requires very strong fields. For instance the strength of the electric field on a Bohr orbit around a charge  $Ze$  is of order  $eE \sim m^2(Z\alpha)^3$ , i.e., only  $4 \times 10^{-7} m^2$  for hydrogen.<sup>3</sup> However, by performing collisions of heavy nuclei with charges  $Z_1$  and  $Z_2$  such that  $Z_1 + Z_2 > 1/\alpha = 137$  it has been possible to observe electron-positron pair production. This has been carried out for the first time at the Unilac facility at GSI Darmstadt which has been able to reach bombarding energies above the Coulomb barrier for reactions such as  $U+Pb$ ,  $U+U$ , or  $U+Cm$  (about 6 MeV per nucleon for the  $U+Cm$  system).<sup>2,4</sup> A second example is the instability of the Dirac vacuum in the presence of a strong gravitational field, which is also discussed in Ref. 2. This instability leads to a quantum evaporation of black holes by pair creation, which has been investigated in different physical situations, e.g., a nonrotating uncharged black hole described by a Schwarzschild metric<sup>5</sup> or a rotating electrically charged black hole described by a Kerr-Newman metric.<sup>5,6</sup>

A last example, which will be discussed at some length below, is the mechanism of energy deposition by quark-antiquark production in ultrarelativistic collisions. Here the external field is the strong chromoelectric field which develops at the early stage of the collision as a result of gluon exchanges.<sup>7-9</sup> The problem in this case is to perform a reliable calculation of the pair-production rate in order to determine the energy density reached during the reaction and the possible formation of a quark-gluon

plasma. In the calculations of Ref. 7 the pair-production rate was evaluated from Schwinger's formula, which is valid for an infinite and uniform electric field. However, the actual configuration of the field is somewhat different, since the chromoelectric field in a collision is enclosed in the flux tube joining in two receding nuclei. Furthermore, the boundary of the field changes with time and one may thus expect corrections to arise for both finite-size and dynamical effects. The purpose of this paper is to show that these corrections are conveniently evaluated by means of the Balian-Bloch multiple-reflection expansion of the Green's functions.<sup>10,11</sup> A preliminary account of the method was presented in a recent Rapid Communication.<sup>12</sup>

In a series of papers<sup>10</sup> Balian and Bloch have constructed approximation schemes of Green's functions in terms of classical paths. They have first investigated the density of modes for the wave equation in a cavity of arbitrary shape. In this case they were able to express the density as a sum over all closed trajectories involving multiple reflections at the boundary. Each closed classical trajectory of length  $L$  provides an oscillating contribution  $\sin(kL)$  to the density of states  $\rho(k)$ . When the surface is smooth the successive terms decrease rapidly. Sharp peaks result out of the interference between different paths. An interesting feature of the expansion is that its first term represents a volume contribution while the next two terms correspond, respectively, to surface and curvature corrections. In a subsequent paper Balian and Bloch have generalized their method in order to build an expansion of the Green's function  $G(\mathbf{r}, \mathbf{r}')$  for a Schrödinger particle in a smooth potential.<sup>11</sup> In this case dominant contributions to  $G$  arise from multiple reflections of the wave emitted at  $\mathbf{r}'$  upon the caustic which is the three-dimensional analog of the turning point. Closed paths of zero length yield the familiar Thomas-Fermi expression for the density of states, together with a smooth correction, while higher-order terms provide an oscillating contribution which reflects the shell structure in the spectrum.

In the following we shall show how the Balian-Bloch expansion can be combined with Schwinger's proper time method to investigate pair production by an external

field. Our paper is organized as follows. In Sec. II we derive a general expression for the pair-production rate up to one reflection in the Balian-Bloch expansion. In Sec. III we consider the specific case of a boundary parallel to the direction of the electric field while Sec. IV discusses the case of a moving boundary perpendicular to the field. A discussion of these formulas in the context of ultrarelativistic collisions is presented in Sec. V while Sec. VI contains a summary of our main conclusions.

## II. THE PRODUCTION RATE UP TO ONE REFLECTION

Let us consider a quantized Dirac field coupled to a classical external Abelian potential  $A_\mu(x)$  described by the interaction Lagrangian

$$\mathcal{L}_I(x) = -e\bar{\psi}(x)\gamma^\mu\psi(x)A_\mu(x). \quad (1)$$

The probability to remain in the ground state, i.e., the probability of emitting no pairs, is given by

$$P = |\langle 0|S|0\rangle|^2, \quad (2)$$

where  $S$  is the  $S$  matrix

$$S = T \exp \left[ i \int d^4x \mathcal{L}_I(x) \right], \quad (3)$$

and  $T$  the time-ordering operator. The probability  $P$  can also be written as

$$P = \exp \left[ - \int d^4x w(x) \right], \quad (4)$$

where

$$w(x) = 2 \operatorname{Im} \mathcal{L}_{\text{eff}}(x). \quad (5)$$

In Eq. (5)  $\mathcal{L}_{\text{eff}}(x)$  is the one-loop effective Lagrangian density,<sup>1</sup> which includes all orders in the external field (but neglects self-interactions of the matter fields). The quantity  $w(x)$  can be interpreted as the pair-production rate per unit time and unit volume at the space-time point  $x = (x_0, x_1, x_2, x_3)$ . This interpretation, however, is valid only in the case of a large volume and a uniform system. In other cases only integrated rates are meaningful.

A convenient integral representation of the one-loop effective Lagrangian is that of Schwinger:<sup>1</sup>

$$\mathcal{L}_{\text{eff}}(x) = \frac{i}{2} \int_0^\infty \frac{ds}{s} e^{-im^2s} \operatorname{Tr} \langle x | e^{iHs} | x \rangle. \quad (6)$$

In this equation the mass  $m$  of the fermions is supposed to contain a small negative imaginary part and  $H$  is the  $4 \times 4$  matrix

$$H = (p - eA)^2 + \frac{e}{2} \sigma_{\mu\nu} F^{\mu\nu}, \quad (7)$$

with the usual notation  $\sigma_{\mu\nu} = i[\gamma_\mu, \gamma_\nu]/2$ . Since the first term in  $H$  is a multiple of the  $4 \times 4$  unit matrix the trace in Eq. (6) is easily carried out. In the case of an external electric field of strength  $E$  along the third axis the only nonvanishing components of the field-strength tensor  $F_{\mu\nu}$  are  $-F_{30} = +F_{03} = E$  and we find that

$$\operatorname{Tr} \exp \left[ i \frac{e}{2} s \sigma_{\mu\nu} F^{\mu\nu} \right] = 4 \cosh(seE). \quad (8)$$

We are thus left with the evaluation of matrix elements of the form

$$U(x, x'; s) = \langle x | \exp(iH_0 s) | x' \rangle, \quad (9)$$

where  $H_0$  is the operator

$$H_0 = (p - eA)^2. \quad (10)$$

The matrix element (9) can be represented in terms of the Feynman path integral<sup>13,14</sup>

$$U(x, x'; s) = \int_{x(0)=x'}^{x(s)=x} \mathcal{D}[x(\tau)] \exp\{iS[x(\tau)]\}, \quad (11)$$

where the action  $S$  is defined by

$$S[x(\tau)] = \int_0^s L[x(\tau)] d\tau. \quad (12)$$

In Eq. (12) the Lagrangian density  $L$  is

$$L = -\frac{1}{4} \dot{x}_\mu \dot{x}^\mu - eA^\mu \dot{x}_\mu = p_\mu \dot{x}^\mu - H_0. \quad (13)$$

A first approximation to the functional integral (11) can be obtained by performing a stationary phase evaluation which gives

$$u(x, x'; s) = \left[ \frac{1}{2\pi i} \right]^2 \det^{1/2}(D^{\mu\nu}) \exp(iS_c). \quad (14)$$

In this equation  $S_c$  is the classical action  $S_c(x', x; s)$  corresponding to a trajectory starting at  $x'$  at time zero and ending at  $x$  at time  $\tau = s$ . The quantity  $D^{\mu\nu}$  is the  $4 \times 4$  matrix<sup>15</sup>

$$D^{\mu\nu} = \partial^2 S_c / \partial x_\mu \partial x'_\nu. \quad (15)$$

Note that Eq. (14) does not involve an infinite-dimensional matrix but rather a  $4 \times 4$  determinant.

Equation (14) actually corresponds to the lowest-order term in the Balian-Bloch expansion of  $U(x, x'; s)$  which involves no reflection at the field boundary. In Ref. 12 we showed that the next term involves a single reflection on the field boundary at a point  $y$  and a time  $s_1$  such that the total action  $S_1 + S_2 = S_c(x', y; s_1) + S_c(y, x; s - s_1)$  is stationary. The corresponding contribution to the matrix element  $U(x, x'; s)$  is

$$U_1(x, x'; s) = (2\pi e^{i\pi/2})^2 \exp[i(S_{1c} + S_{2c})] \times \left[ \frac{1}{2\pi i} \right]^4 \det^{1/2}(D_1 D_2 D_3^{-1}), \quad (16)$$

where  $D_1$ ,  $D_2$ , and  $D_3$  are the following  $4 \times 4$  matrices:

$$\begin{aligned} D_1^{\mu\nu} &= \partial^2 S_{1c}(x', y; s_1) / \partial y_\mu \partial x'_\nu, \\ D_2^{\mu\nu} &= \partial^2 S_{2c}(y, x; s - s_1) / \partial x_\mu \partial y_\nu, \\ D_3^{\mu\nu} &= \partial^2 (S_{1c} + S_{2c}) / \partial y_\mu \partial y_\nu. \end{aligned} \quad (17)$$

The previous determinants satisfy the relation

$$\det(D_1 D_2 D_3^{-1}) = \det(-D_4), \quad (18)$$

where

$$D_4^{\mu\nu} = \partial^2(S_{1c} + S_{2c}) / \partial x_\mu \partial x'_\nu. \quad (19)$$

Equations (14) and (16) require the knowledge of the classical action defined by Eq. (12). For a constant electric field in the  $x_3$  direction, this action is given by

$$\begin{aligned} S_c(x, x'; s) = & \frac{eE}{4} \coth(eEs) [-(x_0 - x'_0)^2 + (x_3 + x'_3)^2] \\ & + \frac{eE}{2} (x_0 x'_3 - x_3 x'_0) \\ & + \frac{1}{4s} [(x_1 - x'_1)^2 + (x_2 - x'_2)^2]. \end{aligned} \quad (20)$$

### III. SURFACE EFFECTS FOR A BOUNDARY PARALLEL TO THE FIELD

From now on we shall consider only contributions involving no reflection or terms with one reflection. These contributions are indeed proportional to the volume and to the surface of the system, respectively. Two (or more) reflection terms would correspond to curvature (or higher-order) corrections. In Ref. 12 we considered the case of an electric field parallel to the third axis localized in the half-space  $x_1 \leq R$ . In this case the optimization of the total action with respect to the reflection point leads to the values

$$S_{1c} = S_{2c} = \frac{1}{2s} (R - x_1)^2. \quad (21)$$

The one-reflection correction to the effective Lagrangian is thus

$$\begin{aligned} \mathcal{L}_{\text{eff}}^1 = & -\frac{1}{8\pi^2} \int_0^\infty \frac{ds}{s^2} \left[ eE \coth(eEs) - \frac{1}{s} \right] \\ & \times e^{-ims^2} e^{i(R-x_1)^2/s}. \end{aligned} \quad (22)$$

To calculate the imaginary part of the integral in Eq. (22), we first perform the change of integration variable  $\tau = is$ . This gives

$$\begin{aligned} \mathcal{L}_{\text{eff}}^1 = & \frac{1}{8\pi^2} \int_0^{i\infty} \frac{d\tau}{\tau^2} \left[ eE \cot(eE\tau) - \frac{1}{\tau} \right] \\ & \times e^{-m^2\tau - (R-x_1)^2/\tau}, \end{aligned} \quad (23)$$

where the integration is 'along the contour  $C_1$  in Fig. 1. However, since the integral along the contour  $C_2$  goes to zero when its radius becomes large, integrations along the contours  $C_1$  and  $C_3$  in this figure give equal contributions. Furthermore, since the integrand along the real axis is real, the only nonvanishing contributions to  $\text{Im}\mathcal{L}_{\text{eff}}^1$  arise from the essential singularity at the origin and the simple poles occurring at  $\tau_n = n\pi/eE$  for  $n=1, 2, \dots$ . Let us first show that the contribution  $I_0$  arising from the singularity at the origin vanishes. Indeed by performing the change of variable  $\tau = \epsilon \exp(i\theta)$  we find

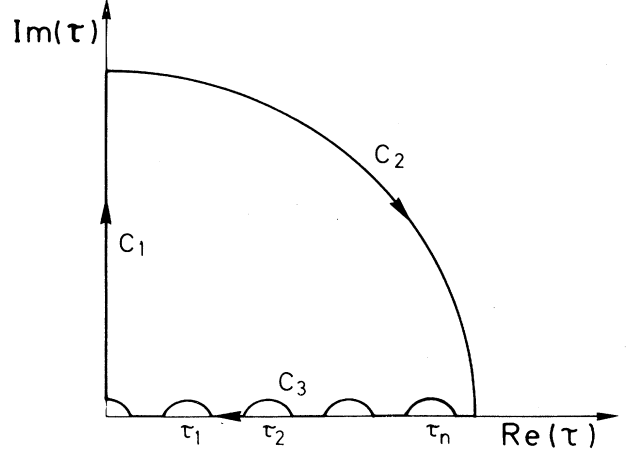


FIG. 1. Contours of integration for evaluating the surface term in the effective Lagrangian  $\mathcal{L}_{\text{eff}}^1$  given by Eq. (22).

$$I_0 = \frac{i}{3} e^2 E^2 \int_0^{\pi/2} \exp[-e^{-i\theta}(R-x_1)^2/\epsilon] d\theta. \quad (24)$$

The imaginary part of this integral is given by an integral sine function

$$\text{Im}I_0 = -(e^2 E^2/3) \text{si}[(R-x_1)^2/\epsilon] \quad (25)$$

which vanishes when  $\epsilon$  goes to zero. We are thus left with the sum of residues at the poles. This gives the following formula for the pair-production rate per unit time and unit volume in the region  $x_1 \leq R$ :

$$\begin{aligned} w(x) = & \frac{e^2 E^2}{4\pi^3} \sum_{n=1}^{\infty} \frac{1}{n^2} \exp\left[-\frac{n\pi m^2}{eE}\right] \\ & \times \left[ 1 - \exp\left[\frac{-eE}{n\pi}(R-x_1)^2\right] \right]. \end{aligned} \quad (26)$$

The first term in the large square brackets corresponds to Schwinger's formula<sup>1</sup> which gives a production rate  $w_0$  proportional to the volume. The second term gives a contribution  $w_1$  which is important only near the boundary at  $x_1 = R$  where it cancels the first one.

In Figs. 2 and 3 we display the ratio  $(w_1 + w_0)/w_0$  as a function of the distance  $d = R - x_1$  from the boundary, for various values of the electric field strength. Figure 2 corresponds to a fermion mass  $m = 10$  MeV, while Fig. 3 corresponds to  $m = 200$  MeV. From these figures we see that surface effects lead to a significant reduction of the Schwinger pair-production rate near the boundary of the field. As an illustrative example (to be discussed later in Sec. V) for a distance  $d = 1$  fm from the surface and for a field strength  $eE = 1$  fm<sup>-2</sup>, the reduction is 80% for a mass  $m = 10$  MeV and 70% for  $m = 200$  MeV. The corresponding figures become 35% and 25% for a field strength  $eE = 5$  fm<sup>-2</sup>.

Equation (26) can be applied to the case of an infinite flux tube in the  $x_3$  direction with a radius  $R$  in the transverse direction. By integrating Eq. (26) over the trans-

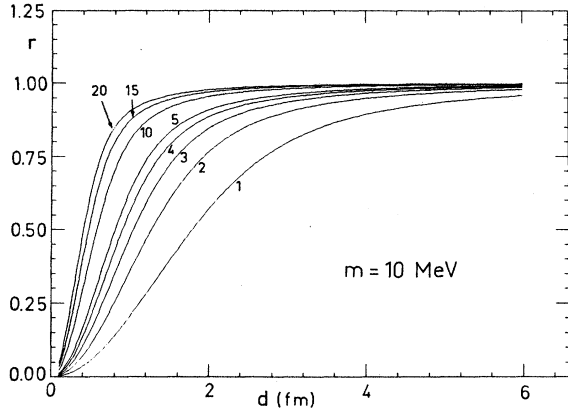


FIG. 2. Ratio  $r$  of the total production rate (volume plus surface contributions) to the volume contribution, for a boundary parallel to the field as a function of the distance  $d$  to the boundary. The fermion mass is  $m = 10$  MeV and the various curves correspond to different strengths of the electric field  $eE$  ( $\text{fm}^{-2}$ ).

verse coordinates  $x_1$  and  $x_2$  we find the following expression for the probability of pair creation per unit time and unit length:

$$\int w(x) dx_1 dx_2 = \pi R^2 \frac{e^2 E^2}{4\pi^3} \times \sum_{n=1}^{\infty} \frac{1}{n^2} \exp\left[-\frac{n\pi m^2}{eE}\right] \times \left[1 - \Phi\left[R\left(\frac{eE}{n\pi}\right)^{1/2}\right]\right], \quad (27)$$

where the function  $\Phi$  is related to the error function

$$\Phi(u) = -\frac{1}{u^2} [1 - \exp(-u^2)] + \frac{\sqrt{\pi}}{u} \text{erf}(u). \quad (28)$$

Since near the origin  $\text{erf}(u) \approx 2u/\sqrt{\pi}$  we find  $\phi(0) = 1$  and the surface term  $\phi$  thus cancels exactly the volume

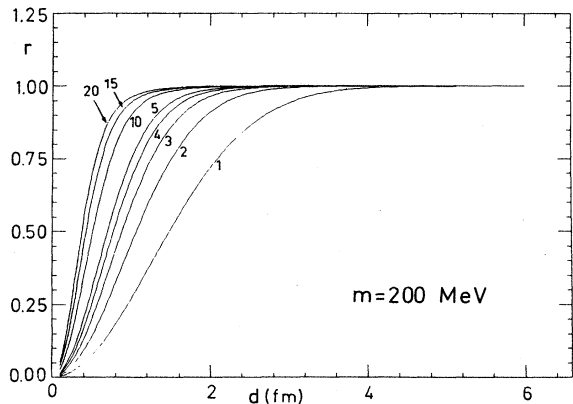


FIG. 3. Same as Fig. 2 for a fermion mass  $m = 200$  MeV.

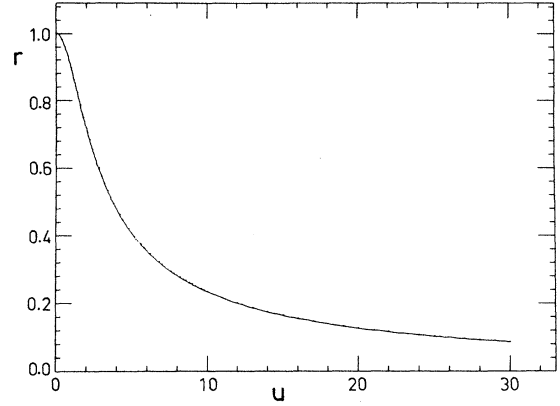


FIG. 4. Ratio  $r$  of surface to volume contributions for pair production in a cylinder of radius  $R$  as a function of the dimensionless variable  $u = R\sqrt{eE/\pi}$ .

term in the limit of a small tube. On the contrary, if we have a large tube, then  $\text{erf}(u) \approx 1$ ,  $\phi \approx +\sqrt{\pi}/u$  and surface effects thus become negligible as soon as  $R \gg \sqrt{\pi/eE}$ . The ratio of surface-to-volume contributions is graphed as a function of the dimensionless variable  $u = R\sqrt{eE/\pi}$  in the case  $m = 0$  in Fig. 4.

#### IV. SURFACE EFFECTS FOR A BOUNDARY PERPENDICULAR TO THE FIELD

Schwinger's proper-time method is explicitly Lorentz invariant as it treats all space-time coordinates  $x_0, x_1, x_2, x_3$  on the same footing. It is thus equally well adapted to handle boundaries in space, time, or in both space and time. In this section we will apply this method to study pair production in an electric field of the form

$$E_x = 0, \quad E_y = 0, \quad E_z = E\theta(vx_0 - x_3). \quad (29)$$

Unlike the previous section we now have to consider reflections occurring at the moving boundary  $x_3 = vx_0$ . This leads to a modification in the argument of the last exponential in Eq. (22) arising from the total action  $S_1 + S_2$ . It is straightforward to check that the reflection still occurs at  $\tau = s/2$  and that the determinants in Eq. (16) remain unchanged. The result for the one-reflection correction to the effective Lagrangian is found to be

$$\mathcal{L}_{\text{eff}}^1(x) = -\frac{1}{8\pi^2} \int_0^\infty \frac{ds}{s^2} \left[ eE \coth(eEs) - \frac{1}{s} \right] \times \exp\left[ -im^2s + ie\frac{E}{2}d^2 \coth\left(\frac{eEs}{2}\right) \right], \quad (30)$$

where

$$d^2 = \gamma^2(vx_0 - x_3)^2 \quad (31)$$

with the usual notation  $\gamma = 1/(1 - v^2/c^2)^{1/2}$ . In the static case  $v = 0$  Eq. (30) still holds and in this case  $d$  is mere-

ly the distance to the boundary. The evaluation of the imaginary part of  $\mathcal{L}_{\text{eff}}^1$  given by Eq. (30) is more difficult than in the case of a boundary parallel to the field. Indeed an important difference is that the singularities occurring at  $\tau = 2n\pi/eE$  are now essential singularities so that the method used in the previous section is no longer applicable.

To simplify let us consider the case  $m = 0$ . In order to evaluate the integral (30) numerically we first perform the change of integration variable  $t = \coth(eEs/2)$  which yields

$$\text{Im}\mathcal{L}_{\text{eff}}^1 = -\frac{1}{8\pi^2} e^2 E^2 \int_1^\infty \phi(t) \sin\left(\frac{eE}{2} d^2 t\right) dt, \quad (32)$$

where the function  $\phi(t)$  is

$$\phi(t) = \frac{1}{(t^2 - 1) \left[ \ln \frac{t+1}{t-1} \right]^2} \left[ t + \frac{1}{t} - \frac{2}{\ln \frac{t+1}{t-1}} \right]. \quad (33)$$

The function  $\text{Im}(\mathcal{L}^1 + \mathcal{L}^0)/\text{Im}\mathcal{L}^0$  is plotted in Fig. 5 as a function of the dimensionless variable  $d\sqrt{eE}$ . For large values of the dimensionless parameter  $d\sqrt{eE}$  the asymptotic behavior of  $\text{Im}\mathcal{L}_{\text{eff}}^1$  is found to be

$$\text{Im}\mathcal{L}_{\text{eff}}^1 \simeq -\frac{1}{8\pi^2} e^2 E^2 \frac{\sin(eEd^2/2)}{\ln(eEd^2/2)} + O\left(\frac{1}{\ln^2(eEd^2/2)}\right) \quad (34)$$

while at short distances it is given by

$$\text{Im}\mathcal{L}_{\text{eff}}^1 \simeq -\frac{e^2 E^2}{48\pi} + \frac{eE^2}{8\pi^2} \left[ \frac{eEd^2}{2} \right] c \quad (35)$$

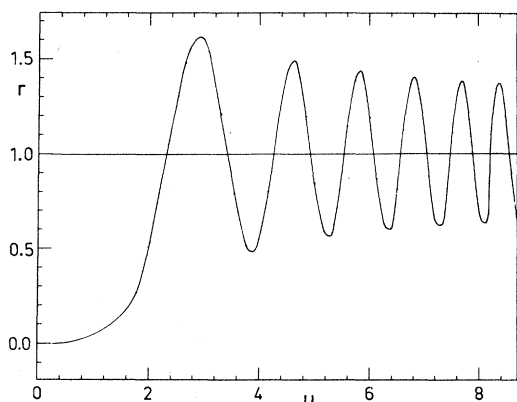


FIG. 5. Ratio  $r$  of the total production rate (volume plus surface contributions) to the volume contribution for a moving boundary ( $x_3 = vx_0$ ) perpendicular to the field, as a function of the dimensionless variable  $u = d(eE)^{1/2}$ . The fermion mass is  $m = 0$ . The ratio  $r$  is small and negative near  $u = 0$  [cf. Eq. (36)]. This may result from our semiclassical approximation.

with

$$c = \frac{1}{3} - \int_1^\infty [t\phi(t) - \frac{1}{3}] dt \simeq -0.10. \quad (36)$$

Note that the first term in Eq. (35) is simply  $-\text{Im}\mathcal{L}^0$  so that the surface term cancels the volume term on the boundary exactly.

From Eq. (34) surface corrections away from the boundary of the field vanish only logarithmically. Although the corresponding decrease is weaker than it was in Eq. (26) one should remember that in the present case the relevant variable  $d$  is the distance to the boundary dilated by a Lorentz factor  $\gamma$ . As a consequence surface corrections vanish for a boundary moving at the speed of light. This result can easily be understood as a consequence of causality. Indeed classical trajectories starting from an arbitrary point  $x$  in space-time will never be able to reach such a boundary. As a result the contribution of the term with one reflection vanishes in this case.

By comparing Figs. 2, 3, and 5 it may be noted that the pair-production rate exhibits oscillations as a function of the distance to the boundary when this boundary is perpendicular to the field. No such oscillations occur for a boundary parallel to the field. This difference can be understood by considering the value of the optimal action  $S_{1c} + S_{2c}$  occurring in Eq. (16). Indeed one finds, for the first case,

$$S_{1c} + S_{2c} = \frac{eE}{2} \coth\left(\frac{eEs}{2}\right) d^2 \quad (37)$$

while in the second case Eq. (21) gives

$$S_{1c} + S_{2c} = \frac{(R - x_1)^2}{s}. \quad (38)$$

Large values of  $s$ , associated with the long trajectories which produce sharp oscillations in the Balian-Bloch method, are thus suppressed in the second case and not in the first. Indeed, these large values contribute a factor  $\exp(iS_{1c} + iS_{2c}) \simeq \exp(ieEd^2/2)$  in the first case and 1 in the second case.

In the special case  $v = 0$  finite-size effects in the Schwinger pair-production mechanism have been calculated exactly by Wang and Wong<sup>16</sup> who solved the Dirac equation in a linear potential in terms of hypergeometric functions. This calculation provides directly a quantity of physical interest, namely, the production rate  $P$  per unit time, transverse area, transverse momentum, and energy interval, whereas our method yields only the rate  $w(x)$  per unit time and unit volume. A detailed comparison between the two results is possible but requires calculations of integrated rates as functions of the volume  $V$  of the system in both cases. A rough comparison, however, can be performed with the approximate rate  $w(x)$  build by Wang and Wong. Keeping in mind the approximations involved, and the fact that a finite value of the mass is used in Ref. 16, we only conclude that there is a qualitative agreement between our results and those of Wang and Wong. In particular we also find large deviations from Schwinger's result for finite systems especially at the field boundary where surface contributions cancel

the volume term. Away from the boundary we obtain sharper oscillations than in Ref. 16.

### V. ENERGY DEPOSITION IN ULTRARELATIVISTIC COLLISIONS

Ultrarelativistic heavy-ion collisions have been successfully described<sup>7,17</sup> by means of the flux-tube model introduced by Low<sup>8</sup> and Nussinov<sup>9</sup> for hadron-hadron collisions (except for the target and projectile mass dependence mentioned below). In this model the two Lorentz-contracted nuclei are described as two color charged capacitor plates and the strong color field between them polarizes the vacuum by production quark-antiquark pairs. The energy deposition in the associated flux tube is subsequently determined by calculating the pair-production rate using Schwinger's formula, which is valid for a uniform infinite electric field. With the results of the previous sections it is interesting to study how the boundaries in the longitudinal and transverse directions of the tube modify the energy deposition. The corrections to Schwinger's formula depend on the radius  $R$  of the tube, on the strength  $eE$  of the chromoelectric field, and on the speed  $v$  of the nuclei in their center-of-mass frame (i.e., on the incident energy).

The NA38 experiment at CERN used 200 GeV per nucleon  $^{16}\text{O}$  and  $^{32}\text{S}$  beams. In these collisions the Lorentz factor  $\gamma$  to be used in Eq. (31) is about 6. For lead-lead collisions at the same energy  $\gamma$  is about 10. According to the results of the previous section, surface effects due to the presence of the boundary in the longitudinal direction become small beyond 0.2 fm from the nuclei for  $\gamma = 10$  and a field strength  $eE = 1 \text{ fm}^{-2}$ . Longitudinal surface effects would be even smaller for the value  $eE = 5 \text{ fm}^{-2}$  adopted in Ref. 16.

Finite-size effects in the transverse direction lead to more important corrections. Indeed, in the flux-tube model of heavy-ion collisions the radius of the tube is typically of the size of 1 fm rather than the size of the nucleus. This is because the spatial variations in color orientation which occur during the color-charging process have a coherence length in the radial direction which is approximately the size of a nucleon.<sup>18</sup> The collision thus leads to the formation of a configuration of neighboring tubes with multiple colors whose transverse size is about 1 fm (which has been called a color rope by Biro, Nielson, and Knoll<sup>18</sup>). Evidence for a transverse size of about 1 fm is substantiated by the values of the average transverse momenta observed in the Helios and NA35 experiments.<sup>19,20</sup>

From the results in Fig. 4 surface effects in the case of a flux tube with a radius  $R = 1 \text{ fm}$  reduce significantly the pair-production rate per unit time and unit length.

Indeed the corresponding reduction is 90% for a field strength  $eE = 1 \text{ fm}^{-2}$  and is still 25% for a field strength  $eE = 15 \text{ fm}^{-2}$ . Such corrections may explain why observed multiplicities in the central rapidity region vary like  $A_T^{1/3} A_P^{2/3}$  (where  $A_P$  and  $A_T$  denote the projectile and target mass, respectively)<sup>21</sup> while the flux-tube model with Schwinger's formula predicts an  $A_T^{1/6} A_P^{5/6}$  dependence [see Eq. (17) of Ref. 17]. If this is the case it would be important to use heavy nuclei in order to reach large energy densities in ultrarelativistic collisions. Indeed for  $A_P = A_T = A$  the field  $eE$  scales like  $A^{1/3}$  (Refs. 7, 17, and 18). Therefore, if we assume that a typical field strength  $eE = 5 \text{ fm}^{-2}$  is reached in  $^{32}\text{S} + ^{32}\text{S}$  collisions, we find from Fig. 4 that the rate of pair production (which is related to the rate of energy deposition) will be multiplied by a factor of about 5 for  $^{208}\text{Pb} + ^{208}\text{Pb}$  collisions. This makes the perspective of developing 200 GeV per nucleon lead beams at CERN especially attractive.

### VI. CONCLUSION

The Schwinger proper-time method combined with the Balian-Bloch multiple-reflection expansion of Green's functions has been demonstrated to be a powerful and elegant tool to investigate corrections to the Schwinger pair-production formula. Indeed it allows one to work out analytically the case of static boundaries parallel to the field or perpendicular to the field, as well as boundaries which evolve with time. We have shown that finite-size corrections are large and almost cancel the volume term within a distance of order  $1/(eE)^{1/2}$  from the boundary, where  $E$  is the field strength. Finite-size corrections are reduced when the field boundary moves with a velocity  $v$  and vanish as a consequence of causality when  $v = c$ . In the case of ultrarelativistic nuclear collisions we argued that energy deposition by pair production was significantly reduced as compared to Schwinger's formula because of the transverse dimension of the chromoelectric flux tube. We have pointed out that in order to reach high energy densities in ultrarelativistic collisions it is of great interest to develop beams of heavy nuclei since the large field involved imply a reduction of surface corrections too.

### ACKNOWLEDGMENTS

One of the authors (C.M.) wishes to thank the Direction des Recherches et Etudes Techniques (DRET) for financial support. We are most grateful to J. P. Blaizot, C. Gerschel, J. Hüfner, and T. Matsui for stimulating discussions. We also wish to thank Gil Gatoff for his constructive criticism as well as for proof reading of the manuscript. Division de Physique Théorique is Unité Associée au CNRS.

<sup>1</sup>J. Schwinger, Phys. Rev. **82**, 664 (1951).

<sup>2</sup>M. Soffel, B. Müller, and W. Greiner, Phys. Rep. **85**, 51 (1982).

<sup>3</sup>C. Itzykson and J. B. Zuber, *Quantum Field Theory* (McGraw-Hill, New York, 1980), p. 195.

<sup>4</sup>J. Schweppe *et al.*, Phys. Rev. Lett. **51**, 2261 (1983).

<sup>5</sup>S. W. Hawking, Commun. Math. Phys. **43**, 199 (1975).

<sup>6</sup>T. Damour and R. Ruffini, Phys. Rev. Lett. **35**, 463 (1975).

<sup>7</sup>G. Gatoff, A. K. Kerman, and T. Matsui, Phys. Rev. D **36**, 114

- (1987).
- <sup>8</sup>F. E. Low, Phys. Rev. D **12**, 163 (1975).
- <sup>9</sup>S. Nussinov, Phys. Rev. Lett. **34**, 1286 (1975).
- <sup>10</sup>R. Balian and C. Bloch, Ann. Phys. (N.Y.) **60**, 401 (1970); **64**, 271 (1971); **69**, 76 (1972).
- <sup>11</sup>R. Balian and C. Bloch, Ann. Phys. (N.Y.) **85**, 514 (1974).
- <sup>12</sup>C. Martin and D. Vautherin, Phys. Rev. D **38**, 3593 (1988).
- <sup>13</sup>R. P. Feynman, Phys. Rev. **80**, 440 (1950).
- <sup>14</sup>C. R. Stephens, Ann. Phys. (N.Y.) **181**, 120 (1988).
- <sup>15</sup>C. DeWitt-Morette, Ann. Phys. (N.Y.) **97**, 367 (1976).
- <sup>16</sup>R. C. Wang and C. Y. Wong, Phys. Rev. D **38**, 348 (1988).
- <sup>17</sup>A. K. Kerman, T. Matsui, and B. Svetitsky, Phys. Rev. Lett. **56**, 219 (1986).
- <sup>18</sup>T. S. Biro, H. B. Nielsen, and J. Knoll, Nucl. Phys. **B245**, 449 (1984).
- <sup>19</sup>H. W. Bartels, Z. Phys. C **38**, 85 (1988).
- <sup>20</sup>H. Strobele, Z. Phys. C **38**, 89 (1988).
- <sup>21</sup>J. Schukraft, Report No. CERN-EP/88-141 (unpublished).